Electronic Supplementary Material (ESI) for Nanoscale.
This journal is © The Royal Society of Chemistry 2014

Electronic Supplementary Information of

"Plasmonic nanorod arrays of two-segment dimer and coaxial cable with 1 nm gap for large field confinement and enhancement"

Zi-Qiang Cheng,[a] Fan Nan,[a] Da-Jie Yang, [a] Yu-Ting Zhong,[a] Liang Ma,[a] Zhong-Hua Hao,[a] Li Zhou*[a] and Qu-Quan Wang*[ab]

[a] Key Laboratory of Artificial Micro- and Nano-structures of the Ministry of Education, and, School of Physics and Technology, Wuhan University, Wuhan, 430072, P.R.China.

[b] Institute for Advanced Study, Wuhan University, Wuhan 430072, P. R. China

Electronic mail: qqwang@whu.edu.cn; zhouli@whu.edu.cn

1. Influence of barrier layer in AAO on the Raman measurement

The tips of two-segment dimer AuNRs were etched out for avoiding the obstruction of Raman signals by the barrier layer in AAO. As the SEM images shown in Figs. S1a-S1f, the barrier layer is thinned stepwise and the AuNRs are gradually exposed as the etch time increases. The dimer AuNRs are almost protruded out at ~25 min (Figure S1e). When the etching time further increases, e.g., after 30 min (Figure S1f), some pores are empty due to the slipping out of NRs from the pores during the etching. As shown in Figures 1g and 1h, the SERS signal intensity increases upon increasing the etching time and reaches a maximum at the etching time of 25 min. After that, it decreases drastically (etching 30 min) most likely due to the slipping out of NRs as well as the disintegration of the AAO template, leading to the reduction in the number of hot spots and in the absolute amount of AuNR dimers.

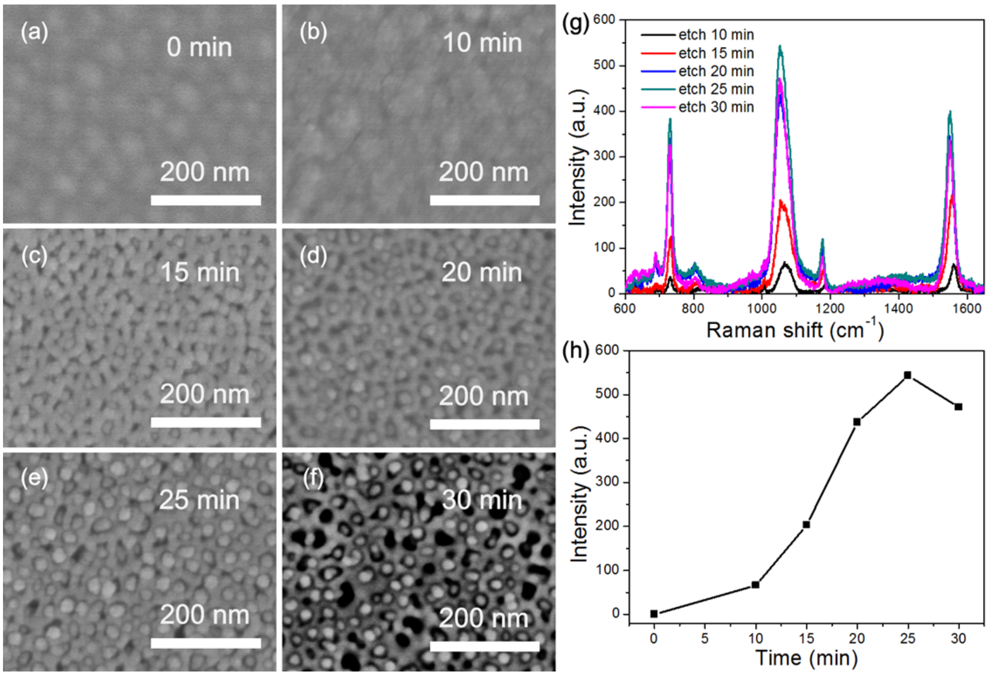

Figure S1. (a)-(f) SEM images of the back-side of the two-segment dimer AuNR arrays. The etching time was set as 0 min, 10 min, 15 min, 20 min, 25 min and 30 min, respectively. (g) The Raman spectra of two-segment dimer samples with different etch time. (h) The Raman intensity profile as a function of the etching time.

2. Residual Raman molecules on the AAO wall

In order to evaluate the Raman signal from the molecules adsorbed on the pore walls of AAO, a reference sample was prepared by immersing the bare AAO template into a 1 mM ethanol solution of 1,4-BDT and then depositing the AuNRs in it. The AAO template was washed several times in ethanol before the AuNR deposition. No Raman signals from the sample were observed before and after the AuNR deposition (Fig. S2), which indicates the Raman molecules adsorbed on the AAO walls were negligible in our experiments.

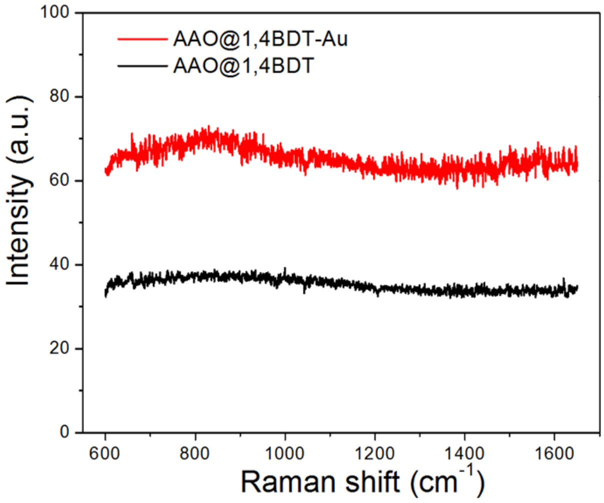

Figure S2. SERS spectra of the bare AAO template that is incubated with 1,4-BDT ethanol solution and washed (black curve), and then is conducted with AuNR deposition (red curve).

3. Stability and reproducibility of two-segment dimer AuNR Raman substrate.

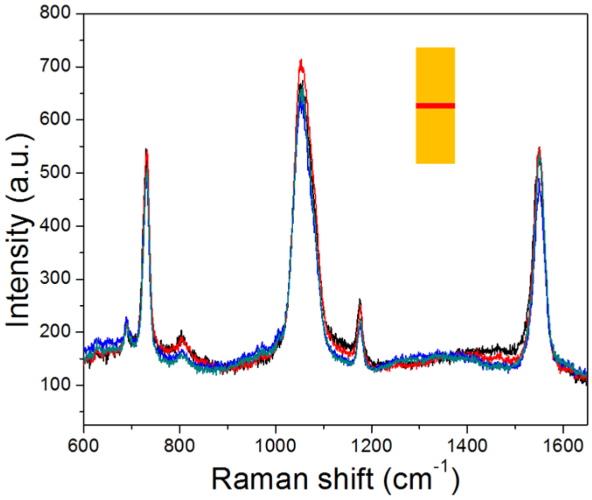

Figure S3. SERS spectra collected at randomly selected spots from the two-segment dimer AuNR array.

4. Extinction and Raman spectra of two-segment Au-Ag dimer NR array.

We also prepared the two-segment Au-Ag dimer NR arrays. The extinction and Raman spectra are shown in Fig. S4. The band at 363 nm in Fig. S4a is corresponding to the transverse surface plasmon resonance of Ag. The SERS signal of the two-segment dimer Au-Ag NRs array is approximation 50 times larger than that of bare AuNRs array.

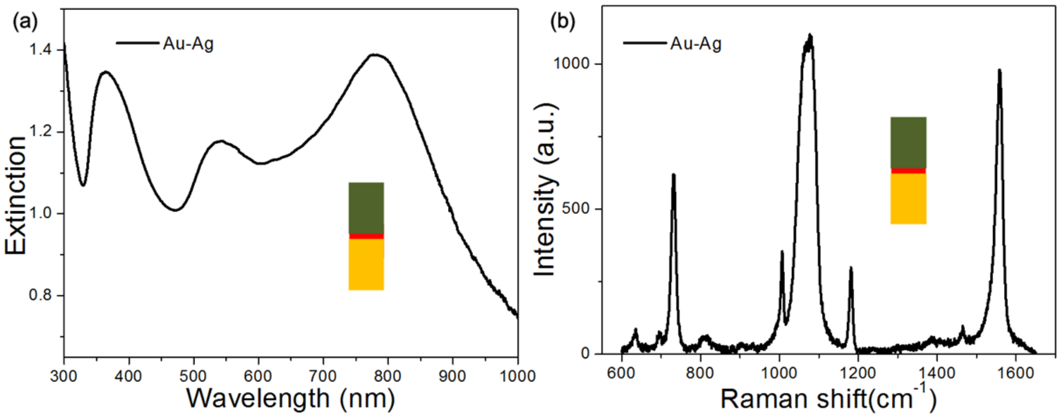

Figure S4. (a) Extinction spectra and (b) Raman spectra of two-segment dimer Au-Ag NR array.

5. Deposition time dependent L-SPR of AuNR arrays

The rod-length and L-SPRs could be adjusted and fine controlled by the deposition time. As shown in Fig. S5, the L-SPR wavelength is stable for the one-segment AuNR arrays with same deposition time.

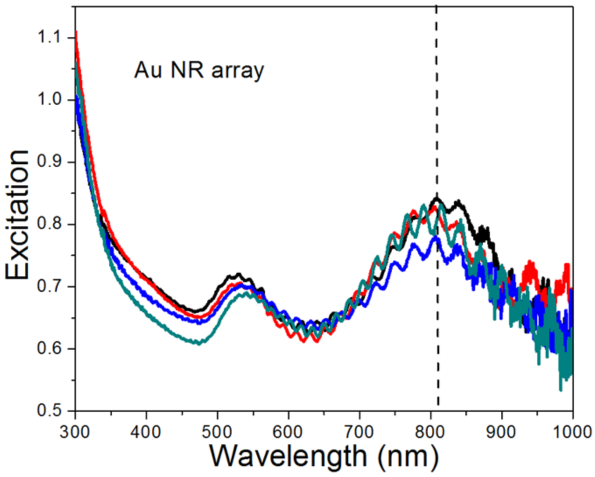

Figure S5. Extinction spectra of four different one-segment Au NR array samples with same deposition time.

6. Extinction spectra of two-segment dimer AuNR arrays with different length ratio L_1/L_2 of two segments.

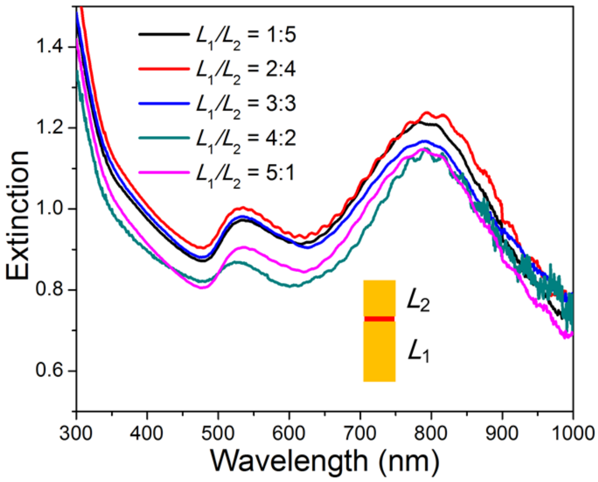

Figure S6. Extinction spectra of five two-segment dimer Au-Au NR array samples with different length ratio of two segments. The length ratio L_1/L_2 was set as 1:5, 2:4, 3:3, 4:2 and 5:1, respectively.

7. PL spectra of Au NR array and 1,4-BDT solution

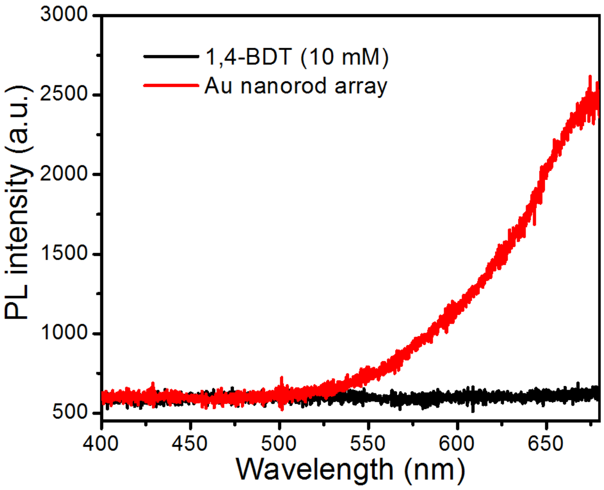

Figure S7. PL spectra of Au NR array and 10 mM 1,4-BDT solution excited by 785 nm laser.

8. Pore widening

Figures S8 shows the SEM images of the mouth-side of AAO templates with and without pore widening and the etched back-side of the AuNR array immersed in an aqueous solution of 5 wt% H_3PO_4. After a 15 min etching, the average pore diameter on the mouth-side is enlarged from ~32 nm to ~45 nm. Meanwhile, the barrier layer on the back-side is etched out an 'air shell' is found around the Au NRs.

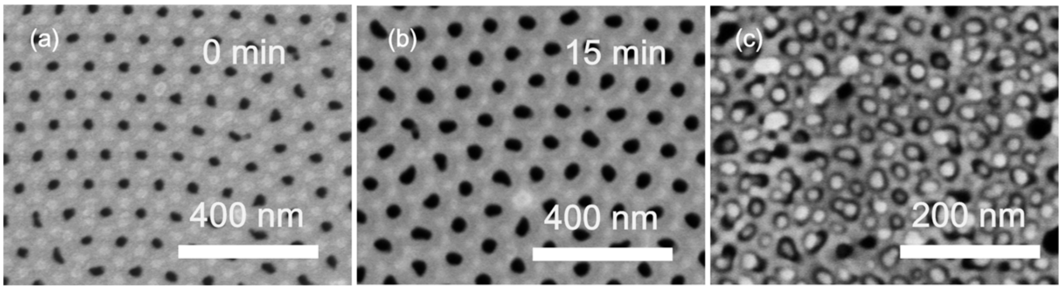

Figure S8. SEM images of the mouth-side of AAO templates without (a) and with (b) pore widening. (c) SEM image of the back-side of AuNR array etched in an aqueous solution of 5 wt% H_3PO_4.

9. HRTEM characterization and EDX analysis of coaxial cable Au@Ag NR

To confirm the composition of the samples further, energy-dispersive X-ray (EDX) analysis was performed on an individual coaxial cable Au@Ag NR with large diameter and length. The spectra in Figure S9 shows Au and Ag peaks in addition to the Cu peaks generated by the copper grid. It can be seen that the main component in the core region (P1) is Au, however that in the shell region (P2) is Ag.

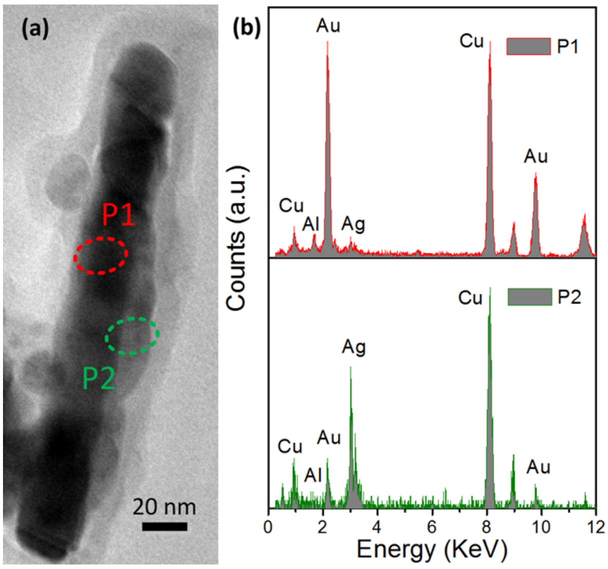

Figure S9 (a) TEM images and (b) EDX of P1 and P2 region of coaxial cable Au@Ag NR.

10. Spectral modulations by wet chemical etching and Ag deposition

In Fig. S10, the L-SPR band is blue-shifted from 806 nm to 780 nm after the pore widening treatment. It is due to the forming of an ‘air shell’ around the AuNRs and then the change of refractive index of the local environment [1-3]. For the Au@Ag cable NRs, the subsequent growth of Ag shells induces the further blue-shift of L-SPR band, which is different from the red-shift for the two-segment Au-Ag dimer NRs. This further blue-shift is caused by the coating of Ag and the reduction of NR aspect ratio. Meanwhile, the L-SPR band shows large enhancement in intensity, which reveals the stronger near-field coupling due to the decreasing inter-rod spacing [1,4].

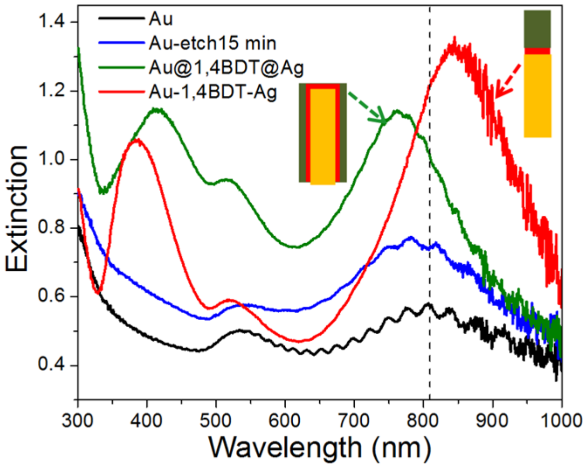

Figure S10. Extinction spectra of one-segment AuNR array without (black line) and with (blue line) pore widening, coaxial cable Au@Ag NR array (green line) and two-segment dimer Au-Ag NR array (red line).

11. Stability and reproducibility of coaxial cable Au@Ag NR Raman substrate

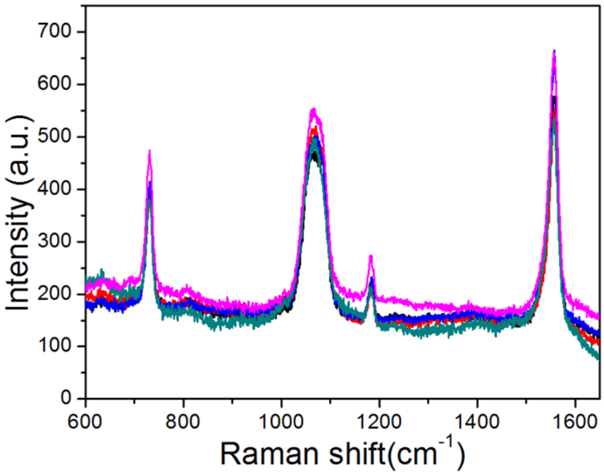

Figure S11. SERS spectra collected at randomly selected spots from the coaxial cable Au@Ag NR substrate.

12. FDTD Simulations

The index of the hole under each rod is taken as 1, and the height of the holes is 500 nm. The NR array has a period a = 100 nm, Au rod diameter d = 30 nm, and gap size $\Delta = 2$ nm. The NRs with holes are placed in an AAO with refractive index 1.6 [5]. For Au NR array, Au rod length L = 76 nm, two-segment dimer NRs $L=L_1+\Delta+L_2$ = 49+2+49 nm, coaxial cable Au@Ag NRs $d = d_{Au}+\Delta+t_{Ag}$ = 30+2+8 nm L= 96 nm.

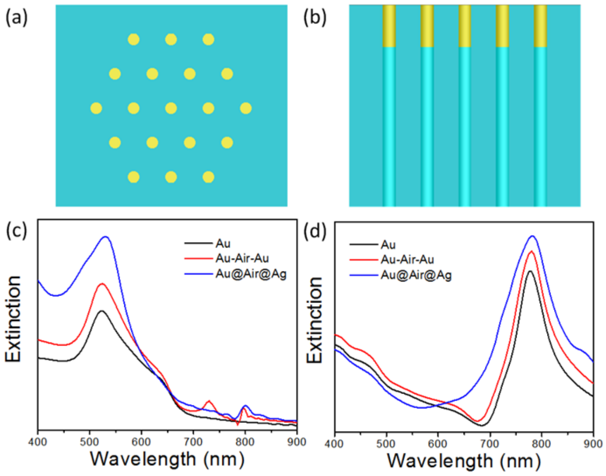

Figure S12. (a) and (b) show top-view and side-view sketches, respectively, of unit cell. (c) and (d) Extinction spectra of the transverse and longitudinal modes for three types nanostructure.

References

[1] P. R. Evans, G. A. Wurtz, R. Atkinson, W. Hendren, D. O'Connor, W. Dickson, R. J. Pollard, and A. V. Zayats, *J. Phys. Chem. C.*, 2007, **111**, 12522-12527.

[2] P. R. Evans, W. R. Hendren, R. Atkinson andR. J. Pollard, *J. Electrochem. Soc.*, 2007,**154**, K79.

[3] W. Dickson, G. Wurtz, P. Evans, D. O'Connor, R. Atkinson, R. Pollard, and A. Zayats, *Phys. Rev. B*, 2007,**76**, 115411

[4] R. Atkinson, W. Hendren, G. Wurtz, W. Dickson, A. Zayats, P. Evans and R. Pollard, *Phys. Rev. B*, 2006,**73**, 235402

[5] F. Nan, Z. Q. Cheng, Y. L. Wang, Q. Zhang, L. Zhou, Z. J. Yang, Y. T. Zhong, S. Liang, Q. H. Xiong and Q. Q. Wang, Sci. Rep., 2014,4, 4839.